Science of the Total Environment 722 (2020) 137755

Contents lists available at ScienceDirect

Science of the Total Environment

journal homepage: www.elsevier.com/locate/scitotenv

An inter-comparative evaluation of PKU-FUEL global SO_2 emission inventory

Jinmu Luo, Yunman Han, Yuan Zhao, Xinrui Liu, Yufei Huang, Linfei Wang, Kaijie Chen, Shu Tao, Junfeng Liu, Jianmin Ma *

College of Urban and Environmental Sciences, Laboratory for Earth Surface Processes, Peking University, Beijing 100871, China

HIGHLIGHTS

- Top-down and bottom-up emission inventories were used to verify PKU-FUEL SO_2 emission inventory.
- Missing SO_2 point sources were identified in PKU-FUEL SO_2 inventory.
- PKU-FUEL provides reliable SO_2 emissions in Asia and Europe.
- OMI is used to improve the performance of PKU-FUEL.
- GEOS-Chem modeling was performed to verify improved PKU-FUEL against measurement.

GRAPHICAL ABSTRACT

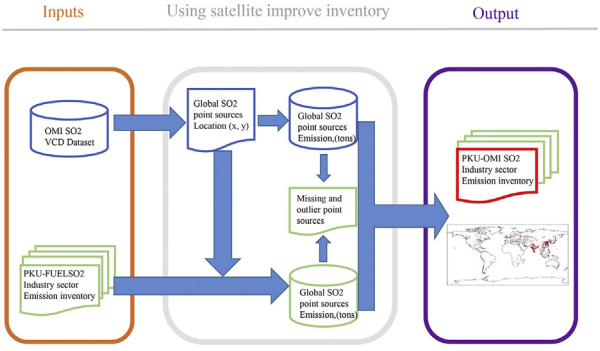

ARTICLE INFO

Article history:
Received 5 January 2020
Received in revised form 3 March 2020
Accepted 4 March 2020
Available online 05 March 2020

Editor: Jianmin Chen

Keywords:
Bottom-up inventory
OMI
PKU-OMI
GEOS-Chem

ABSTRACT

PKU-FUEL is a recently developed gridded global emission inventory for multiple air pollutants that uses a bottom-up approach. The inventory includes data collected monthly for the period of 1960 to 2014 and at a 0.1° × 0.1° latitude/longitude resolution. In an effort to evaluate and improve this emission inventory, the PKU-FUEL Sulfur Dioxide (SO_2) emission inventory was compared to other currently available and widely used global SO_2 emission inventories constructed based on bottom-up and top-down approaches, including CEDS and OMI-HTAP. While PKU-FUEL is capable of capturing SO_2 emissions across the globe and particularly in Asia, it misses 41 industrial point sources globally, accounting for 9.3% of Ozone Monitoring Instrument (OMI) remote sensing-measured industrial point sources. Most of these missing point sources are identified in Latin America, the Middle East (~60%), and some remote places. To improve the PKU-FUEL SO_2 inventory, we applied OMI-measured emissions to sources missing from PKU-FUEL. GEOS-Chem model simulations were performed to evaluate original and improved PKU-FUEL SO_2 inventories against measured SO_2 concentrations across the world. Results were further compared to GEOS-Chem modeled SO_2 concentrations using the CEDS inventory. We show that the modeled SO_2 concentrations determined using both CEDS and improved PKU-FUEL inventories to a large extent corroborate sampled data and that the improved PKU-FUEL performs better for those regions lacking monitoring data.

* Corresponding author.
E-mail address: jmma@pku.edu.cn (J. Ma).

https://doi.org/10.1016/j.scitotenv.2020.137755
0048-9697/

1. Introduction

Anthropogenic emission inventories of air pollutants have been extensively used to help policymakers and modelers predict source-receptor relationships, perform risk assessments, and adapt appropriate regulations for air pollutants of concern (Eder et al., 2009; Ma and Aardenne, 2004; Zhang et al., 2012). Efforts have been made to develop regional and global air pollutant emission inventories over the past two decades, including the Emission Database for Global Atmospheric Research (EDGAR, Janssens-Maenhout et al., 2011), Evaluating the Climate and Air Quality Impacts of Short-Lived Pollutants (ECLIPSE, Stohl et al., 2015), CEDS (Community Emissions Data System (Hoesly et al., 2018), OMI-HTAP (Liu et al., 2018; McLinden et al., 2016), and the Multi-resolution Emission Inventory for China (MEIC, C. Li et al., 2017, M. Li et al., 2017). Some of these inventories cover long time periods but at relatively coarse spatial resolutions (ECLIPSE, Stohl et al., 2015; CEDS, Hoesly et al., 2018) while other inventories have a high spatial resolution but cover relatively short time periods (OMI-HTAP, Liu et al., 2018). These inventories also have their respective advantages and disadvantages based on the collection of emission data, emission-related factors, the precision of spatial proxy data, and the compilation of emission sources. Among these factors, the reliability of point sources featuring emissions from industries depends on the monitored and reported air release (Oda et al., 2010; Ummel, 2012). A lack of accurate monitoring and emission reporting systems for the industrial release of air pollutants in numerous countries and regions has resulted in many missing point sources, compromising the emission inventory's accuracy. For precisely reported point sources, since the same material burned within a point source may be related to different emission factors in different places (Jeon et al., 2010; Werf et al., 2010; Yokelson et al., 2007), the estimated emissions of materials released from a point source may overestimate or underestimate emission levels in different regions. In addition to point sources, non-point sources or diffusive emission datasets are always clustered within a region or country. To establish a gridded emission inventory, one must pinpoint a statistical emission dataset into a gridded emission map. This further requires different surrogates or spatial proxy datasets to map emissions based on, for instance, population density, human activities, and land cover types, introducing additional uncertainty into an emission inventory (Wang et al., 2013). Due to these difficulties, such inventories may report significant biases for certain continents and countries. Within this context, a comparative evaluation of different emission inventories could facilitate the development of a unified inventory that combines the advantages of different emission inventories while mitigating the disadvantages of these inventories. Such an approach could be adopted in the ensemble forecasting of air quality (Petersen et al., 2019). Recently, Peking University of China developed and released a global air emission inventory at a 0.1° by 0.1° latitude/longitude spatial resolution and monthly temporal resolution for 1960 to 2014. The inventory was established using a bottom-up approach (Huang et al., 2014, 2017; Wang et al., 2013). Given difficulties associated with the collection of global emission data, which has resulted in many missing sources, PKU-FUEL is also expected to be subject to biases and uncertainties. However, compared to other global emission inventories developed in Europe and the United States (US) (EDGAR, ECLIPSE, CEDS, and OMI-HTAP), PKU-FUEL may take advantage of more reliable and abundant SO_2 emission data for Asia and China, which account for two-thirds of all SO_2 emissions generated in Asia (Ling et al., 2017). Considering PKU-FUEL, as the first global SO_2 emission inventory applying a high spatial-temporal resolution in China and Asia, the present study involved extensive evaluations of the PKU-FUEL SO_2 emission inventory to provide an alternative emission dataset that may help improve global emission inventories of air pollutants.

Evaluations of emission inventories of air pollutants have been carried out in many previous works (Ding et al., 2017; McLinden et al., 2016; Urbanski et al., 2011; Urbanski and Hao, 2010; Zhao et al., 2011). Two approaches have often been employed within this context. The comparison of different emission inventories is often used to validate an emission inventory (Ding et al., 2017). Another approach involves applying an inventory to an atmospheric chemistry model to predict atmospheric concentrations of air pollutants and then comparing the modeled data with in situ measurements. Here, we adopted both approaches to examine PKU's (Peking University's) global SO_2 emissions inventory.

We first compared PKU-FUEL SO_2 emissions with two widely used global SO_2 emission inventories: CEDS (Hoesly et al., 2018), and OMI-HTAP (Liu et al., 2018; McLinden et al., 2016). We adopted this approach because both inventories were developed based on EDGAR (Crippa et al., 2018), which has been employed extensively in the air quality science community. Regarding the two inventories adopted here to compare to PKU-FUEL, CEDS was developed using a bottom-up technique and OMI-HTAP was established through a combination of top-down and bottom-up approaches (Liu et al., 2018). Considering that OMI-HTAP has been proved superior to bottom-up emission inventories (Liu et al., 2018), this inventory is applied as a reference emission inventory to estimate the uncertainty and reliability of PKU-FUEL SO_2 emissions. In the first instance, we identified and accounted for missing point sources in the two bottom-up inventories through the use of top-down OMI-based SO_2 emissions, which have been successfully utilized to identify global SO_2 point sources (McLinden et al., 2016; Koukouli et al., 2018). We then examined correlations between the PKU-FUEL inventory and the other two inventories (OMI-HTAP and CEDS). GEOS-Chem was used to simulate global SO_2 concentrations using the three SO_2 inventories. The modeled SO_2 concentrations were then compared to the measured SO_2 air concentration data to evaluate PKU-FUEL's performance relative to the other two inventories.

2. Data and methods

2.1. PKU-fuel

The PKU-FUEL (http://inventory.pku.edu.cn/, last accessed on 25 September 2019) global emission inventories were developed using a bottom-up approach at a 0.1° by 0.1° latitude/longitude resolution and monthly temporal resolution for 1960 to 2014. PKU-FUEL provides a series of global emission inventories for carbon dioxide (CO_2), carbon monoxide (CO), nitrogen oxides (NO_X), ammonia (NH_3), sulfur dioxide (SO_2), fine particulate matter (PM_{10} and $PM_{2.5}$), total suspended particles (TSP), carbonaceous speciation (BC, OC), and 16 polycyclic aromatic hydrocarbons (PAHs). In total, 64 to 88 (except CH4) individual sources (i.e., sector and fuel combinations) from the PKU emission inventory were taken into account. Among these air pollutants, SO_2 emissions are mainly generated through fuel and biomass burning and from combustion processes and activities.

2.2. Omi-HTAP

As a top-down technique, satellite remote sensing has been used for the global environmental monitoring of vegetation coverage, water resources, atmospheric variables, and air pollutants among other variables. In recent years, the technique has been increasingly employed to improve air emission inventories constructed using bottom-up approaches (Li et al., 2018; Liu et al., 2018; McLinden et al., 2016). One such technique is based on the Ozone Monitoring Instrument (OMI). The OMI is a Dutch-Finnish sensor aboard the National Aeronautics and Space Administration's (NASA's) Earth Observing System (EOS) Aura satellite launched in July 2004. The OMI is an ultraviolet/visible (UV/VIS) nadir solar backscatter spectrometer that provides global coverage over a single day. The spatial resolution of the OMI is 13 km × 24 km. The OMI was designed to detect levels and trends of ozone and other trace gases in the troposphere across the globe (Levelt et al., 2006). Methods and techniques used for the retrieval of

atmospheric trace gases using the OMI have been reported elsewhere (Krotkov et al., 2006; Li et al., 2013; Veefkind et al., 2006).

Fioletov et al. (2015) developed an emission detection algorithm to estimate the OMI-based SO_2 burden and emission catalogs of roughly 500 sources worldwide, which was extended to measure OMI-based SO_2 emissions. Due to restrictions on the OMI's spatial resolution (13 km × 24 km), the OMI-derived SO_2 emission inventory can identify only emission sources of >30 Kt yr^{-1} (Fioletov et al., 2015). The OMI also cannot identify types of emission sources and can determine only the locations and volumes of significant emissions sources. OMI-based emissions have been combined with a conventional bottom-up HTAP emission inventory referred to as OMI-HTAP (HTAP v2.2, available at http://edgar.jrc.ec.europa.eu/htap_v2, last accessed 28 September 2019) to take less significant sources into account (Liu et al., 2018). Since HTAP v2.2 provides data for only 2008 and 2010, even though OMI-HTAP provides annual SO_2 emissions for 2005 to 2014, in most years of this period OMI-HTAP's reported emissions are identical to the OMI SO_2 emissions developed by Fioletov et al. (2015) except for 2008 and 2010.

2.3. CEDS

CEDS (Community Emissions Data System) is a new global emission inventory for anthropogenic, chemically reactive gases, aerosols, and aerosol precursors based on energy consumption (Hoesly et al., 2018). CEDS provides gridded SO_2 emissions for 1750 to 2014. Similar to PKU-FUEL, CEDS is a monthly emission inventory but with a relatively coarse spatial resolution of 0.5° × 0.5° latitude/longitude. More detailed information about CEDS can be found at http://www.globalchange.umd.edu/ceds/ (last accessed on 4 September 2019). After August 2018, CEDS emissions replaced EDGAR data as the default global anthropogenic inventory used in the GEOS-Chem modeling community (http://wiki.seas.harvard.edu/geoschem/index.php/CEDS_anthropogenic_emissions, last accessed on 4 September 2019).

2.4. Improved PKU-FUEL

We use OMI-based SO_2 emissions to improve the PKU-FUEL SO_2 inventory (Zhong et al., 2019). Note that OMI estimate point sources mainly originate from industry emissions, so we account for only SO_2 emissions generated from industry sectors. We first incorporated the missing point sources identified in Section 3.1 into PKU-FUEL. To do so, we allocated an OMI point source emission rate to grid cells within a circle with a 50 km radius centered on the point source. We then replaced gridded PKU-FUEL emission rates within the same circles with OMI-retrieved emissions in the loop. When the emission strength of the PKU-FUEL SO_2 inventory for any grid was ten times higher or lower than that of OMI-retrieved emissions, these emission rates were also replaced with OMI-retrieved emissions using the same approach as that employed for the treatment of missing point sources. A similar approach was also applied to improve SO_2 emissions estimates for China (Koukouli et al., 2018). Given that OMI-retrieved SO_2 emissions for the US are more accurate than those for other regions (Fioletov et al., 2015), any SO_2 point source emissions from PKU-FUEL for the US two times higher or lower than the OMI-derived emissions were replaced with OMI-retrieved emissions. After these steps, 41 missing point sources were incorporated into PKU-FUEL industrial sources, and 22 large point sources and 145 small sources were modified by OMI-retrieved SO_2 emissions.

2.5. GEOS-Chem

The GEOS-Chem model was used to evaluate and compare original and modified PKU-FUEL and CEDS inventories. GEOS-Chem is a global-scale three-dimensional (3-D) model for tropospheric chemistry driven by assimilated meteorological observational data collected through NASA's GMAO Modern-Era Retrospective Analysis for Research and Application (MERRA) meteorological dataset. The chemical mechanism of GEOS-Chem covers over 80 species and 300 reactions with detailed photo-oxidation schemes for major anthropogenic hydrocarbons and isoprene, which are calculated with the Fast-J algorithm (Bey et al., 2001). More information about physics and chemistry schemes of GEOS-Chem can be found at http://wiki.seas.harvard.edu/geos-chem/index.php/Main_Page (last accessed on 25 August 2019). In the present study, GEOS-Chem 12.3.2 was used at a grid resolution of 4° × 5° latitude/longitude. The model was run in 2014 with 2013 as adopted the spin-up year. Three model scenarios were set to simulate SO_2 air concentrations using the three emission inventories. The first model scenario is the default scenario using the GEOS-Chem-recommended CEDS inventory as initial conditions (referred to the CEDS run). The second and third scenarios incorporate the original and modified PKU-FUEL inventories into the model run and are referred to as the PF1 and PF2 runs, respectively. The modeled concentrations were compared to available in situ SO_2 measurements collected across the globe to examine the performance of the original and modified PKU-FUEL and CEDS. It should be noted that GEOS-Chem model grid cells with a 4° × 5° lat/lon resolution often cannot match the location of a PAH sampling site. We collected modeled mean concentrations averaged over the 4 adjacent grid points of a grid cell covering all available sampling sites. We then estimated correlations between the modeled mean concentrations and measured mean concentrations averaged over sampling sites within the model grid cell.

2.6. Sampled SO_2 air concentrations

Monitored SO_2 air concentrations for 2014 were collected to verify GEOS-Chem-modeled concentrations taken from three model scenario runs. We selected 2014 for our emission and model result evaluations because China started its official operation of its air quality sampling network across the country in 2014 (http://www.cnemc.cn/, last accessed on 5 August 2019). Other SO_2 in situ measurement data were mostly available for the US (https://aqs.epa.gov/aqsweb/airdata/download_files.html#Daily, last accessed on 5 August 2019) and Europe (http://aidef.apps.eea.europa.eu, last accessed on 5 August 2019). Routinely sampled SO_2 concentrations were collected from the China National Environmental Monitoring Center (http://www.cnemc.cn/, last accessed on 5 August 2019).

3. Results

3.1. Missing point sources

As mentioned in Section 2.4, the PKU-FUEL SO2 emission inventory has been improved using satellite remote sensing data as a robust way to monitor surface activities and evaluate an emission inventory of air pollutants (such as PKU-FUEL) occurring near the surface (McLinden et al., 2016). We used a smoothing technique (Fioletov et al., 2011) to interpolate OMI pixels into 0.05° x 0.05° lat/lon grid cells, which has been demonstrated to be capable of identifying point sources with emission rates of higher than 30 Kt yr^{-1}. For small-scale point sources with SO_2 emission rates of <30 Kt yr^{-1}, either the emission signal is too weak to be detected or such sources cannot produce a statistically significant signal in OMI data (Fioletov et al., 2015). In this case, the OMI cannot correctly capture SO_2 emissions. The smoothing technique was employed to enhance pixel resolutions to discern point sources or hot spots from the reconstructed emission maps (Fioletov et al., 2011). It should be noted that the OMI occasionally receives false signals from snow- or desert-covered underlying surfaces. This problem can be solved by Google Earth to distinguish real emission sources and reject untrustworthy point sources. For further details, please refer to (McLinden et al., 2016). For point sources not identified in an emission

inventory, OMI remote sensing data serve as a very useful tool for identifying those missing point sources.

As noted above, OMI-HTAP combines top-down and bottom-up emissions to identify significant and less significant sources (Liu et al., 2018). The inventory was further employed to examine the PKU-FUEL and CEDS emission inventories. Fig. 1 illustrates OMI-derived SO_2 emissions generated from global point sources for 2005. As is shown, significant emission sources are located in eastern and southern Asia and especially in the Northern China Plain (NCP). A recent investigation of the MSAQSO2L4 project (Multi-Satellite Air Quality Sulfur Dioxide Database Long-term L4, available at https://disc.gsfc.nasa.gov/, last accessed on April 7, 2019) adopting an OMI top-down technique found 514 point sources globally. Excluding natural emissions generated from volcanic eruptions, 443 industrial point sources were selected to examine missing point sources in PKU-FUEL.

As multiple point sources are often located within the same grid cell at a 50 km × 50 km resolution (Fioletov et al., 2011), these sources are taken as a single point source within a grid cell with a 50 km radius. We further determined that when the emission rate from a point source in PKU-FUEL and CEDS was lower than 5 Kt/yr but higher than 30 Kt/yr as estimated by the OMI, this point source was considered a missing point source. Fig. 2 illustrates the number of missing point sources in PKU-FUEL (Fig. 2a) and CEDS (Fig. 2b) emission inventories for five continents: the Americas, Asia, Africa, Europe, and Oceania. Since there are only a few point sources for South America, we combine South America and North America and collectively refer to these as the Americas. In general, a large number of missing point sources were found for the Americas and Asia for the PKU-FUEL and CEDS inventories and a small number were found for Europe, Africa, and Oceania in the two bottom-up inventories. As is shown in Fig. 2, Mexico, Central America, and Middle Eastern countries account for a larger number of missing point sources, likely due to limited air quality measurement and emission data. PKU-FUEL missed 41 industrial point sources globally, accounting for 9.3% of the global total (443). Among these 41 missing point sources, 17 are located in the Americas, 2 are located in Africa, 8 are located in Europe, 12 are located in Asia, and 2 are located in Oceania. CEDS missed 34 point sources, accounting for 8% of the global total, and 14 are located in the Americas, 1 are located in Africa, 7 are located in Europe, 11 are located in Asia, and 1 is located in Oceania. These results suggest that CEDS performed better than PKU-FUEL in terms of missing emission sources identified from OMI remote sensing data. This was expected because the CEDS-SO_2 inventory consulted and scaled SO_2 emission data with available emission inventories from across the globe, e.g., EMEP for Europe (EMEP, 2016), MEIC for China (C. Li et al., 2017, M. Li et al., 2017), and the US (the USEPA). Traditionally, the allocation of a point source within a spatial grid cell depends on industrial emission release and statistical emission data collection at and near grid cells and on the selection of proper proxies and surrogates such as human population density, GDP statistics, night light indexes, etc. to allocate an emission rate to a grid cell. A lack of data creates significant errors in a gridded emission inventory. This often occurs in less developed countries/regions and remote areas where emission and in situ air quality measurements are not routinely reported or collected. The better performance of CEDS as featured by its fewer missing point sources for Europe, North America, Russia, and Asia is likely attributable to emission data reporting legislation applied within the OCED (Organization for Economic Co-operation and Development) and in Annex I countries (Janssens-Maenhout et al., 2011) and to emission data sharing between EDGAR and REAS (Regional Emission Inventory in Asia, Ohara et al., 2008; Kurokawa et al., 2013).

3.2. Temporal trends and spatial similarities

Fig. 3 shows the temporal variation in annual SO_2 emissions (Kt/yr) for PKU-FUEL, CEDS, and OMI-HTAP, respectively, summed for each of the five continents. Overall, yearly total emissions from the three inventories exhibit similar trends, showing declining SO_2 emissions for the Americas (dominated by emissions in North America) and Europe due to the operation of an emission control strategy for the past several decades. SO_2 emissions listed in PKU-FUEL show better agreement with CEDS for the Americas and Europe but are higher for Africa, Asia, and Oceania. As opposed to what is observed in developed countries, however, in Asia and Africa, PKU-FUEL SO_2 emissions increased from 2000 to 2005, but this trend levelled off in Asia after 2005 as shown by annual emissions given by PKU-FUEL. In the Americas and Europe, summed annual SO_2 emissions from the three inventories correspond reasonably well with emission strength and temporal variations. Nevertheless, PKU-FUEL yields somewhat higher SO_2 emissions after 2008 (Fig. 3a and b). The good performance of these inventories for the Americas and Europe is attributable to good air quality sampling data and SO_2 release reporting systems from industrial point sources (Janssens-Maenhout et al., 2011). For Africa and Asia, PKU-FUEL yields higher emissions than CEDS and OMI-HTAP. Given that China accounted for two-thirds of Asia's SO_2 emissions (Ohara et al., 2008; Shen et al., 2016; Ling et al., 2017), the higher annual emissions averaged over Asia can be primarily attributed to emission estimates for China (Fig. 3e). Underestimated SO_2 emissions for Asia given by CEDS and OMI-HTAP are primarily attributable to their underestimations of SO_2 emissions for China as shown in Fig. S1 of the Supplementary Materials, likely due to the use of different desulfuration efficiency values (Zhong

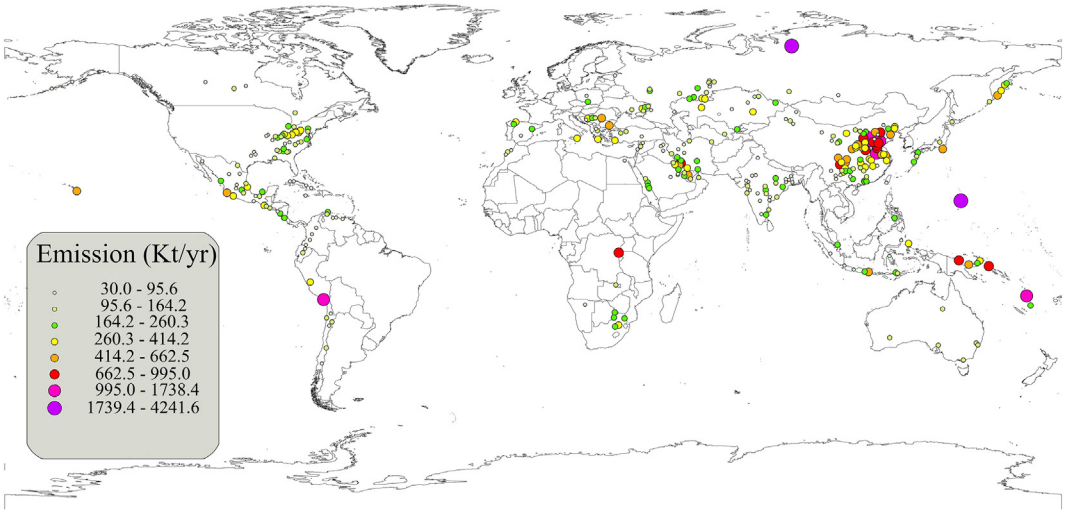

Fig. 1. Global point source emissions (Kt yr^{-1}) for 2005.

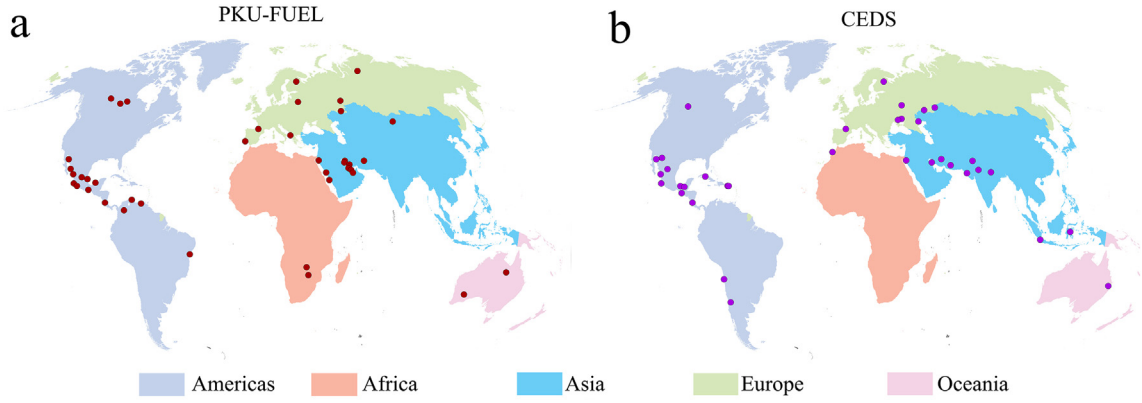

Fig. 2. Number of missing industrial point sources in PKU-FUEL (a) and CEDS (b) SO_2 emission inventories for the five considered continents for 2005.

et al., 2019). In this sense, PKU-FUEL may yield a better estimate of SO_2 emissions for Asia than the other inventories because it was constructed based on the direct use of more information on SO_2 release, emission factors, and spatial proxy data for China. In other words, CEDS might underestimate SO_2 emissions for China. For Oceania, CEDS reports considerably lower SO_2 emissions than PKU-FUEL and OMI-HTAP (Fig. 3c). Unlike PKU-FUEL and OMI-HTAP, which present nearly constant or slightly increasing SO_2 emissions, CEDS shows a decline in SO_2 emissions from 2008.

We further used the nonparametric Mann-Kendall Test (M-K test) to estimate gridded SO_2 emission trends recorded in PKU-FUEL. To compare spatial similarities, the M-K test was also applied in a trend analysis of the CEDS and OMI-HTAP SO_2 inventories for 2005 to 2014. For relatively short time series of emission data, the M-K test is useful for assessing the statistical significance of time series trends and is suitable for application to non-normally distributed and censored data that are not influenced by abnormal values (Yue and Pilon, 2011). Fig. 4 illustrates M-K test-estimated temporal trends for PKU-FUEL, OMI, and CEDS SO_2 point source emissions for 2005 to 2014. Most point sources showing decreases in SO_2 emissions are located in the eastern US and eastern China. Sources showing increasing trends are found in India, the Middle East, and some central Asian and Central American countries. PKU-FUEL also reports an increase in SO_2 emissions for Japan. Although SO_2 emissions have not been officially updated in Japan since 2008, the OMI-derived SO_2 emissions show decreasing trends for most areas of Japan (Fig. 4a). These SO_2 trends closely reflect global economic development, industrialization, and air pollution remediation trends for the past decade. SO_2 emissions increased in almost all less developed countries while they decreased in developed countries. To reduce SO_2 emissions, from 2005 onward the Chinese government has issued and implemented a series of regulations, strategies, and SO_2 control measures, leading to a drastic decrease in SO_2 emissions, particularly in eastern and southern China (Li et al., 2010; Ling et al., 2017; Lu et al., 2011; Shen et al., 2016). This effort is clearly reflected in OMI (Fig. 4a), PKU-FUEL (Fig. 4c), and CEDS (Fig. 4b) SO_2 emissions. India has also been identified as the largest source of anthropogenic emissions of SO_2 in the world in recent years (C. Li et al., 2017, M. Li et al., 2017) in line with our estimated emission trends as shown in Fig. 4.

Considering again OMI-HTAP's superior capacity to capture point emission sources and show better agreement with reported SO_2 sources, we compared PKU-FUEL emission rates with mean emission rates of OMI-HTAP averaged over each of the five continents (Fig. 2). Fig. S2a-e shows correlation diagrams for PKU-FUEL and OMI-HTAP emission rates for 443 industrial point sources across the five continents. As is shown, PKU-FUEL reports lower emissions than the OMI-HTAP inventory for the Americas (Fig. S2a), Africa (Fig. S2d), and Oceania (Fig. S2c), which seems to contradict the results given in Fig. 3 presenting higher SO_2 emissions from PKU-FUEL than from OMI-HTAP for these two continents. This is likely attributable to the fact that unlike OMI-HTAP, PKU-FUEL includes several missing point sources or mistakenly allocates point sources in less developed countries/regions. This further suggests that top-down satellite remote sensing could serve as a useful means to improve a bottom-top inventory.

3.3. Modified PKU-FUEL SO_2 emissions from the OMI

After incorporating industrial emissions into the PKU-FUEL SO_2 emission inventory, spatial changes in the improved PKU-FUEL inventory for 2014 were assessed using the OMI-retrieved emission inventory (Fioletov et al., 2015). Fig. 5 illustrates changes in SO_2 annual emission rates across the globe. Russia experienced the most significant increase in emissions at 2524 Kt in 2014. This significant increase in SO_2 emissions could be attributed to the identification of a large industrial point source in Norilsk, Russia (69°N, 88°E), which has been considered one of the largest industrial emission sources in the world but has not been reported in previous emission reporting systems (Bauduin et al., 2014). Other regions with marked increases in emissions are located in the Middle East, Central America, and Southeast Asia. In contrast, we observed a significant decrease in SO_2 emissions of 12,120 Kt from the modified inventory for China for 2014. India and North America also show decreasing emissions of 145 Kt to 2739 Kt as shown in Fig. 5. Table S1 presents mean absolute and relative errors of SO2 emissions for the original PKU-FUEL and CEDS and OMI SO2 inventories for the five continents. As is shown, the PKU-FUEL inventory yields relatively larger statistical errors for Africa and the Americas with most missing sources located in less developed countries.

3.4. Emission inventory evaluation

The updated PKU-FUEL SO_2 emission inventory was first compared to SO_2 point source emissions for across the US for 2005 collected by the US Environmental Protection Agent (USEPA). The dataset includes 29 point sources. Fig. S3 shows correlation diagrams for USEPA reported point source emissions and the PKU-FUEL inventory, the updated PKU-FUEL inventory after adding missing point sources, and CEDS SO_2 emissions for the US. While the PKU-FUEL and CEDS inventories do not statistically significantly match the USEPA data, CEDS performed better than PKU-FUEL. After adding missing sources and improving source strengths, the correlation between the updated PKU-FUEL inventory and USEPA reported emissions increased from −0.1651 (Fig. S3) to 0.7721.

Detailed emission inventory evaluations were carried out using the GEOS-Chem model. We first added gridded SO_2 emissions into the GEOS-Chem chemistry transport model to predict gridded hourly and daily SO_2 concentrations in the air. We then evaluated the modeled concentrations by comparing simulated data with monitored ambient concentrations. When modeled concentrations were consistent with the monitored data, we assumed that the emission inventory should be as

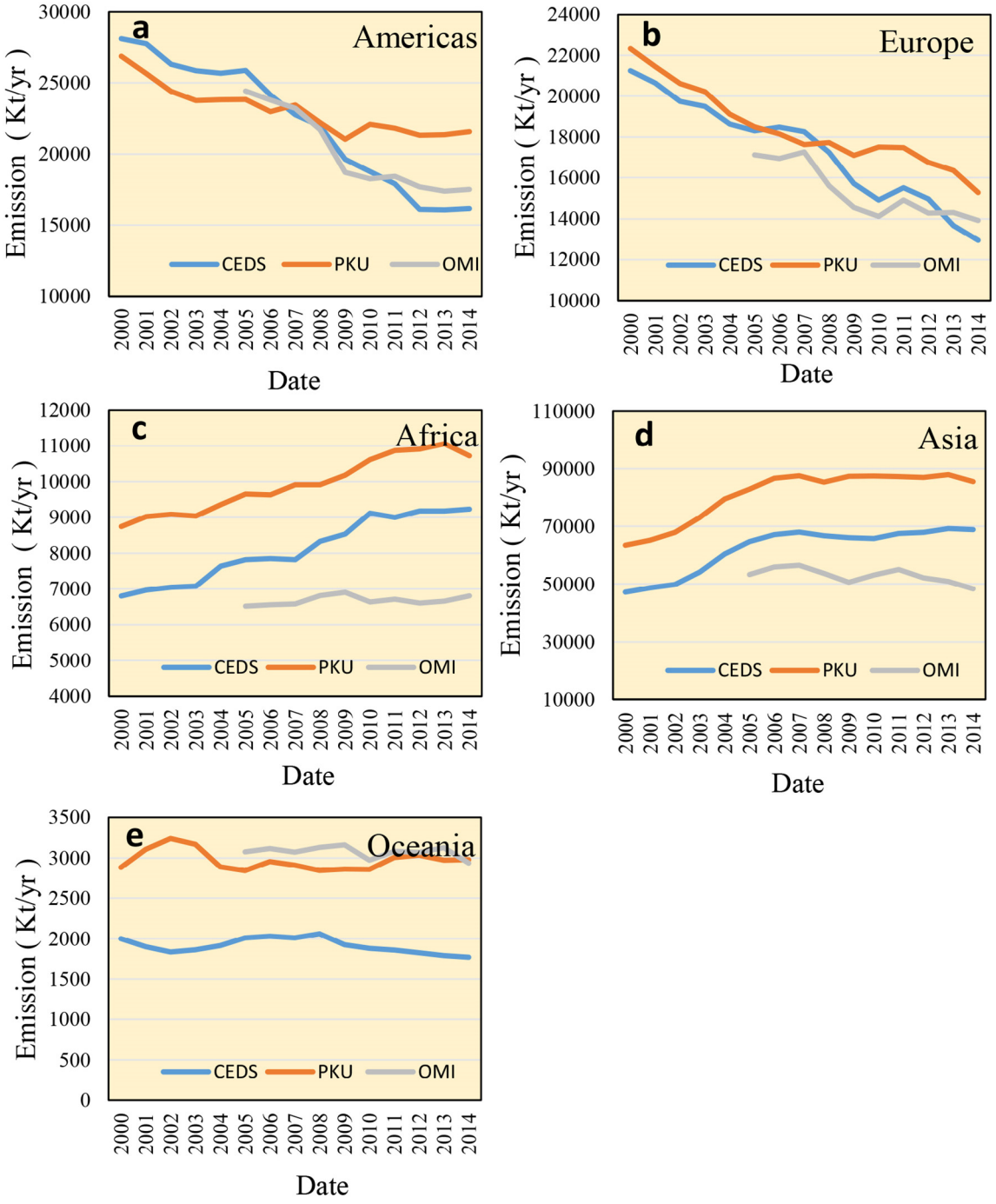

Fig. 3. Temporal variation of annual SO_2 emissions (Kt/yr) from three inventories for the five continents studied (Fig. 3a–e) for 2005 to 2014 for OMI-HTAP and for 2000 to 2015 for the other two bottom-up inventories.

reliable as model inputs of initial conditions of air concentrations. Fig. S4 shows GEOS-Chem-simulated annual SO_2 air concentrations averaged over 2014 for across the globe based on the CEDS inventory (CEDS scenario or background simulation) (Fig. S4a), original PKU-FUEL inventory (PF1 scenario, Fig. S4c), and updated PKU-FUEL inventory (PF2 scenario, Fig. S4b). Overall, the modeled SO2 concentrations exhibit similar spatial patterns with higher SO_2 levels for eastern China and India. However, the PF2 results show concentration "hot spots" in the Middle East, Russia, central Asia, and South Africa relative to the CEDS and PF1 runs. These concentration "hot spots" can be attributed to missing point sources added to the original PKU-FUEL SO_2 inventory. Fig. 6 further displays differences between GEOS-Chem molded SO_2 concentrations derived from the original and updated PKU-FUEL (PKU-OMI) inventories and namely, model scenarios PF1 and PF2 ($=C_{PF2} - C_{PF1}$, where C_{PF1} and C_{PF2} are modeled SO_2 concentrations from PF1 and PF2 scenario runs, respectively). There appear to be no significant differences in modeled air concentrations between the PF1 and PF2 runs for the Americas except for one case in southern Mexico for which PF2 predicts higher SO_2 concentrations, suggesting a missing source in the original PKU-FUEL inventory for this area. The PF1 and PF2 scenario simulations also show higher SO_2 concentrations for China and India than the CEDS scenario simulation (Fig. S5), which is in line with results presented in Fig. 3e showing that CEDS underestimated annual SO_2 concentrations for 2000 to 2014 for Asia given that SO_2 emissions in China and India overwhelm total emissions in Asia. However, the updated PKU-FUEL SO_2 inventory for China reduces SO_2 emissions for eastern

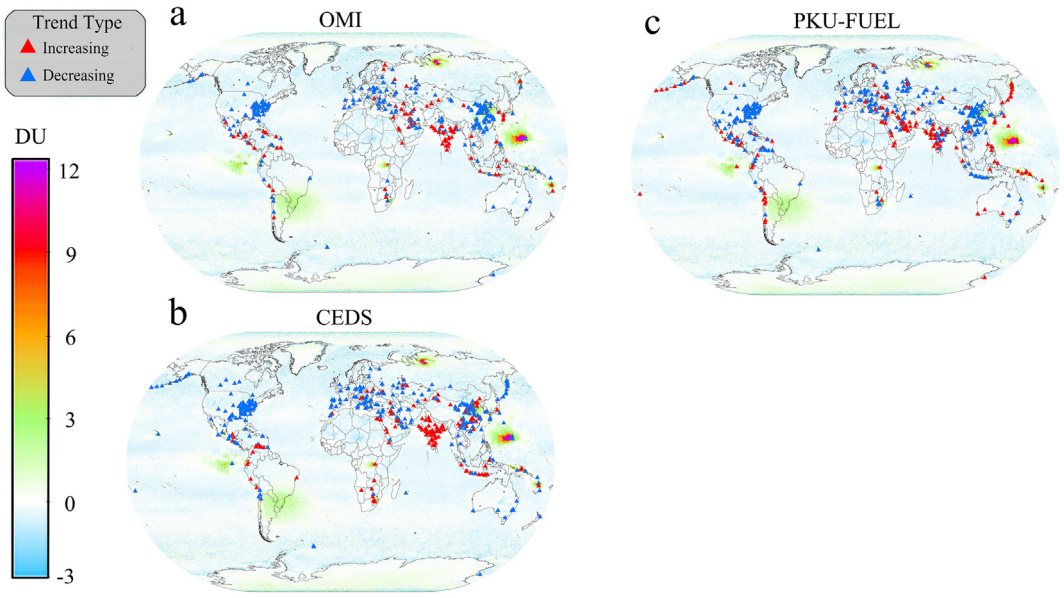

Fig. 4. Trends of SO_2 emissions (Kt/yr) in point sources across the globe from the OMI, PKU-FUEL, and CEDS inventories estimated by the Mann-Kendall Test. Red and blue triangles denote increasing and decreasing point source levels. The background map shows concentrations of OMI-retrieved SO_2 column density (DU) for 2005 as shown in the color bar on the left. a. SO_2 emission trends for 2005 through 2014 from OMI, b. the same data as those given in Fig. 4a but for CEDS, **c**. the same data as those given in Fig. 4a but for PKU-FUEL. (For interpretation of the references to color in this figure legend, the reader is referred to the web version of this article.)

China as shown by the negative value of $C_{PF2} - C_{PF1}$ (Fig. 6). This shows that the original PKU-FUEL inventory might overestimate SO_2 emissions for China.

Fig. 7 shows the correlations between modeled monthly SO_2 air concentrations from PF1 and PF2 model scenarios using original and updated PKU-FUEL inventories and measured concentrations for China, Europe, and the US for 2014, respectively. As is shown, the updated PKU-FUEL inventory did not improve SO_2 simulations for the US and Europe. It even yielded a lower correlation coefficient ($r = 0.26$, $p = 0.03$) than that generated by the original inventory ($r = 0.36$, $p \ll 0.05$) for Europe. As is shown in Fig. 2, no missing point sources of SO_2 were found for the US. As a result, we did not observe a marked difference in correlation coefficients between modeled concentrations from the two PKU-FUEL scenario runs and measured data for the US

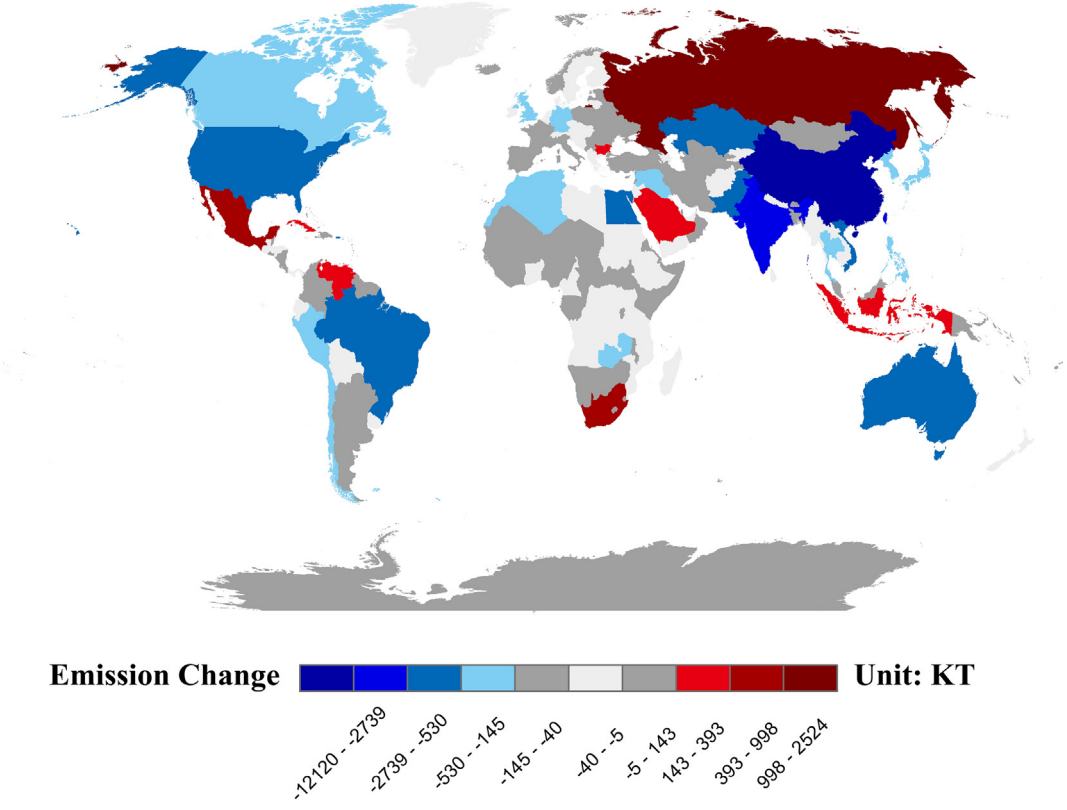

Fig. 5. Changes in country-level emission rates in terms of modified PKU-FUEL SO_2 values after incorporating missing sources retrieved by OMI remote sensing with PKU-FUEL for 2014.

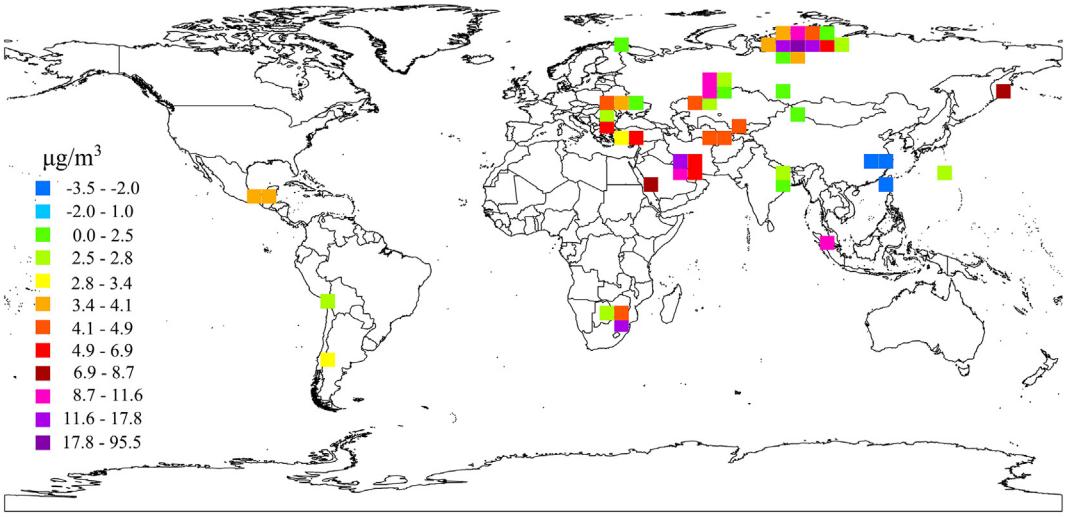

Fig. 6. GEOS-Chem-simulated SO_2 surface concentration differences ΔC_{SO2} (μg/m^3) between PF1 and PF2 model scenario runs using original and updated PKU-OMI SO_2 emission inventories ($\Delta C_{SO2} = C_{PF2} - C_{PF1}$).

as shown in Fig. 7b. We also examined GEOS-Chem-simulated SO2 concentrations using the CEDS emission inventory (CEDS model scenario) against measured data (Fig. S5). The CEDS model scenario more accurately predicted mean SO_2 concentrations for Europe and China than that using original and updated PKU-FUEL data (Fig. S5a and c) but did not perform well for the US ($r = 0.12$, $p \ll 0.05$, Fig. S5b) relative to PKU-FUEL data ($r = 0.27$, $p < <0.05$ Fig. 7c). Table S2 presents mean and relative errors of modeled SO_2 air concentrations derived from the PF1 and PF2 model scenario run and monitored concentrations for China, the US, and Europe for 2014. The application of the updated PKU-FUEL emission inventory to GEOS-Chem reduces the mean absolute errors of modeled concentrations for China and Europe but increases the relative error for Europe. No significant changes in mean absolute and relative errors were found between original and updated PKU-FUEL inventory-derived SO_2 air concentrations for the US, confirming similarities between original and updated PKU-FUEL data for the US due to an absence of missing sources for this country. It should be noted that as shown in Figs. 2 and 6, some missing sources were identified in remote areas. Due to an absence of reliable measurement and reported emission data for these areas, we could not verify the updated PKU-FUEL SO_2 inventory for these areas.

4. Conclusions and discussion

In this study, we examined and evaluated the recently released PKU-FUEL SO_2 global emission inventory. We first compared PKU-FUEL with the OMI-HTAP inventory developed through a combination of bottom-up and top-down approaches. The results were used to identify missing global industrial point sources and emission outliers in PKU-FUEL. These missing sources and outliers were then incorporated into PKU-FUEL SO_2. Updated PKU-FUEL data were then compared to another global SO_2 emission inventory CEDS recommended by the GEOS-Chem modeling community with a smaller number of missing point sources than PKU-FUEL. It was found that PKU-FUEL SO_2 emissions perform differently for different continents, yielding more reliable SO_2 emissions for China and Asia but higher SO_2 emissions for the Americas, Africa, and Oceania than CEDS. Multiple model scenario simulations using GEOS-Chem and the original and updated PKU-FUEL inventories were performed to evaluate the two inventories against sampled SO_2 air concentrations for China, the US, and Europe for 2014. The modeling results reveal that both the original and updated PKU-FUEL inventories performed reasonably well, and the updated PKU-FUEL inventory to some degree improved the modeled SO_2 concentrations for some less developed regions and countries. Given that significant differences between the original and updated PKU-FUEL data were identified for some remote areas, the updated PKU-FUEL inventory might yield more significant improvements for these remote regions, though this was not verified due to a lack of measured SO_2 emissions and concentrations.

As mentioned in Section 2, the PKU-FUEL inventory extends from 1960 to 2014 while OMI remote sensing SO_2 emissions are available only from 2005 onward. Thus, PKU-FUEL cannot be improved using OMI-derived emissions before 2005. While some improvements for 2014 are shown in Fig. 7 and Table S2 for China, Europe, and the US, these improvements are not significant. While remarkable improvements may be achieved for less developed countries and regions as shown in Fig. 6, this cannot be easily verified due to a lack of in situ measurement data for these countries and regions. Hence, if PKU-FUEL were employed to developed countries and regions, for which sufficient SO_2 emission data and measured concentrations are available, the original PKU-FUEL inventory might not need to be modified using OMI-

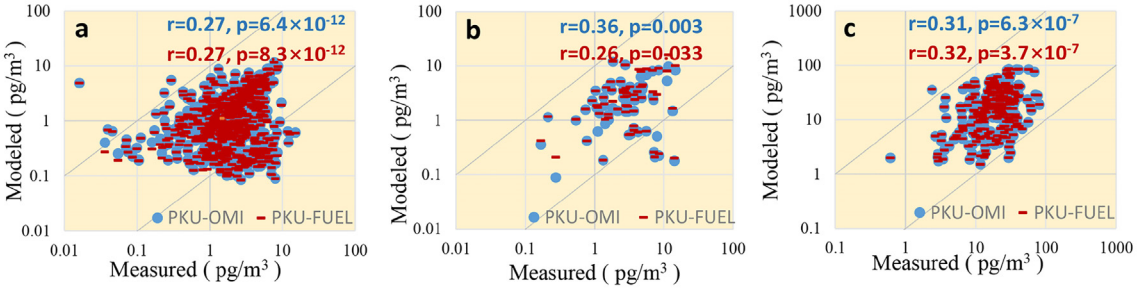

Fig. 7. Correlation diagrams for GEOS-Chem-modeled monthly SO_2 air concentrations for model scenarios PF1 and PF2 incorporating original and updated PKU-FUEL inventories and monitored concentration data for 2014 for China (a), the US (b), and Europe (c).

derived SO_2 emissions. Within this context, the original PKU-FUEL SO_2 emission inventory is equally reliable for 1960 to 2014. Considering its fine spatial resolution (0.1° × 0.1° lat/lon) and period covered (1960 to 2014) relative to OMI-HTAP and CEDS, PKU-FUEL might serve as a useful tool for the air quality modeling community and for policymakers in the assessment and evaluation of air pollution control strategies.

CRediT authorship contribution statement

Jinmu Luo: Writing - original draft, Methodology, Formal analysis. **Yunman Han:** Formal analysis, Visualization. **Yuan Zhao:** Formal analysis. **Xinrui Liu:** Investigation, Data curation. **Yufei Huang:** Formal analysis, Investigation. **Linfei Wang:** Formal analysis. **Kaijie Chen:** Formal analysis. **Shu Tao:** Data curation, Writing - review & editing. **Junfeng Liu:** Writing - review & editing. **Jianmin Ma:** Conceptualization, Formal analysis, Writing - original draft, Funding acquisition.

Declaration of competing interest

The authors declare that they have no known competing financial interests or personal relationships that could have appeared to influence the work reported in this paper.

Acknowledgment

The authors of this article wish to thank the financial support from the National Natural Science Foundation of China (grant number 41977357) and the National Key Research and Development Program of China (grant number 2017YFC0212002). The authors of this paper also wish to thank Dr. V. Fioletov for providing the AMF and 29 USEPA point sources, and precious advice on point sources estimate methods and constructive discussions.

Appendix A. Supplementary data

Supplementary data to this article can be found online at https://doi.org/10.1016/j.scitotenv.2020.137755.

References

Bauduin, S., Clarisse, L., Clerbaux, C., Hurtmans, D., Coheur, P.-F., 2014. IASI observations of sulfur dioxide (SO2) in the boundary layer of Norilsk. J. Geophys. Res. Atmospheres 119, 4253–4263. https://doi.org/10.1002/2013JD021405.

Bey, I., Jacob, D.J., Yantosca, R.M., Logan, J.A., Field, B.D., Fiore, A.M., Li, Q., Liu, H.Y., Mickley, L.J., Schultz, M.G., 2001. Global modeling of tropospheric chemistry with assimilated meteorology: model description and evaluation. J. Geophys. Res. Atmospheres 106, 23073–23095. https://doi.org/10.1029/2001JD000807.

Crippa, M., Guizzardi, D., Muntean, M., Schaaf, E., Dentener, F., van Aardenne, J.A., Monni, S., Doering, U., Olivier, J.G.J., Pagliari, V., Janssens-Maenhout, G., 2018. Gridded emissions of air pollutants for the period 1970–2012 within EDGAR v4.3.2. Earth Syst. Sci. Data 10, 1987–2013. https://doi.org/10.5194/essd-10-1987-2018.

Ding, J., Miyazaki, K., van der A, R.J., Mijling, B., Kurokawa, J., Cho, S., Janssens-Maenhout, G., Zhang, Q., Liu, F., Levelt, P.F., 2017. Intercomparison of NO_x emission inventories over East Asia. Atmospheric Chem. Phys. 17, 10125–10141. https://doi.org/10.5194/acp-17-10125-2017.

Eder, B., Kang, D., Mathur, R., Pleim, J., Yu, S., Otte, T., Pouliot, G., 2009. A performance evaluation of the National Air Quality Forecast Capability for the summer of 2007. Atmos. Environ. 43, 2312–2320. https://doi.org/10.1016/j.atmosenv.2009.01.033.

EMEP, 2016. , Accessed date: 10 October 2019.

Fioletov, V.E., Mclinden, C.A., Krotkov, N., Moran, M.D., Yang, K., 2011. Estimation of SO2 emissions using OMI retrievals. Geophys. Res. Lett. 38, 01. https://doi.org/10.1029/2011GL049402.

Fioletov, V.E., McLinden, C.A., Krotkov, N., Li, C., 2015. Lifetimes and emissions of SO2 from point sources estimated from OMI. Geophys. Res. Lett. 42, 1969–1976. https://doi.org/10.1002/2015GL063148.

Hoesly, R.M., Smith, S.J., Feng, L., Klimont, Z., Janssens-Maenhout, G., Pitkanen, T., Seibert, J.J., Vu, L., Andres, R.J., Bolt, R.M., Bond, T.C., Dawidowski, L., Kholod, N., Kurokawa, J., Li, M., Liu, L., Lu, Z., Moura, M.C.P., O'Rourke, P.R., Zhang, Q., 2018. Historical (1750–2014) anthropogenic emissions of reactive gases and aerosols from the Community Emissions Data System (CEDS). Geosci. Model Dev. 11, 369–408. https://doi.org/10.5194/gmd-11-369-2018.

Huang, Y., Shen, H., Chen, H., Wang, R., Zhang, Y., Su, S., Chen, Y., Lin, N., Zhuo, S., Zhong, Q., Wang, X., Liu, J., Li, B., Liu, W., Tao, S., 2014. Quantification of Global Primary Emissions of PM2.5, PM10, and TSP from Combustion and Industrial Process Sources [WWW Document]. https://doi.org/10.1021/es503696k.

Huang, T., Zhu, X., Zhong, Q., Yun, X., Meng, W., Li, B., Ma, J., Zeng, E.Y., Tao, S., 2017. Spatial and temporal trends in global emissions of nitrogen oxides from 1960 to 2014. Environ. Sci. Technol. 51, 7992–8000. https://doi.org/10.1021/acs.est.7b02235.

Janssens-Maenhout, G., Crippa, M., Guizzardi, D., Muntean, M., Schaaf, E., 2011. EDGAR-HTAP: A Harmonized Gridded Air Pollution Emission Dataset Based on National Inventories.

Jeon, E.-C., Myeong, S., Sa, J.-W., Kim, J., Jeong, J.-H., 2010. Greenhouse gas emission factor development for coal-fired power plants in Korea. Appl. Energy 87, 205–210. https://doi.org/10.1016/j.apenergy.2009.06.015.

Koukouli, M.E., Theys, N., Ding, J., Zyrichidou, I., Mijling, B., Balis, D., Johannes, van der, 2018. A uppdated SO 2 emission estimates over China using OMI/Aura observations. Atmos. Meas. Tech. 11, 1817–1832.

Krotkov, N.A., Carn, S.A., Krueger, A.J., Bhartia, P.K., Yang, K., 2006. Band residual difference algorithm for retrieval of SO/sub 2/from the aura ozone monitoring instrument (OMI). IEEE Trans. Geosci. Remote Sens. 44, 1259–1266. https://doi.org/10.1109/TGRS.2005.861932.

Kurokawa, J., Ohara, T., Morikawa, T., Hanayama, S., Janssens-Maenhout, G., Fukui, T., Kawashima, K., Akimoto, H., 2013. Emissions of air pollutants and greenhouse gases over Asian regions during 2000–2008: regional emission inventory in ASia (REAS) version 2. Atmospheric. Chem. Phys. 13, 11019–11058. https://doi.org/10.5194/acp-13-11019-2013.

Levelt, P.F., Oord, G.H.J.V.D., Dobber, M.R., Malkki, A., Visser, H., Vries, J.D., Stammes, P., Lundell, J.O.V., Saari, H., 2006. The ozone monitoring instrument. IEEE Trans. Geosci. Remote Sens. 44, 1093–1101. https://doi.org/10.1109/TGRS.2006.872333.

Li, C., Zhang, Q., Krotkov, N.A., Streets, D.G., He, K., Tsay, S.-C., Gleason, J.F., 2010. Recent large reduction in sulfur dioxide emissions from Chinese power plants observed by the ozone monitoring instrument. Geophys. Res. Lett. 37. https://doi.org/10.1029/2010GL042594.

Li, C., Joiner, J., Krotkov, N.A., Bhartia, P.K., 2013. A fast and sensitive new satellite SO2 retrieval algorithm based on principal component analysis: application to the ozone monitoring instrument. Geophys. Res. Lett. 40, 6314–6318. https://doi.org/10.1002/2013gl058134.

Li, C., McLinden, C., Fioletov, V., Krotkov, N., Carn, S., Joiner, J., Streets, D., He, H., Ren, X., Li, Z., Dickerson, R.R., 2017. India is overtaking China as the World's largest emitter of anthropogenic sulfur dioxide. Sci. Rep. 7, 14304. https://doi.org/10.1038/s41598-017-14639-8.

Li, M., Zhang, Q., Kurokawa, J.-I., Woo, J.-H., He, K., Lu, Z., Ohara, T., Song, Y., Streets, D.G., Carmichael, G.R., Cheng, Y., Hong, C., Huo, H., Jiang, X., Kang, S., Liu, F., Su, H., Zheng, B., 2017. MIX: a mosaic Asian anthropogenic emission inventory under the international collaboration framework of the MICS-Asia and HTAP. Atmos. Chem. Phys. 17, 935–963. https://doi.org/10.5194/acp-17-935-2017.

Li, M., Klimont, Z., Zhang, Q., Martin, R.V., Zheng, B., Heyes, C., Cofala, J., Zhang, Y., He, K., 2018. Comparison and evaluation of anthropogenic emissions of SO2 and NOx over China. Atmospheric Chem. Phys. 18, 3433–3456. https://doi.org/10.5194/acp-18-3433-2018.

Ling, Z., Huang, T., Zhao, Y., Li, J., Zhang, X., Wang, J., Lian, L., Mao, X., Gao, H., Ma, J., 2017. OMI-measured increasing SO_2 emissions due to energy industry expansion and relocation in northwestern China. Atmospheric Chem. Phys. 17, 9115–9131. https://doi.org/10.5194/acp-17-9115-2017.

Liu, F., Choi, S., Li, C., Fioletov, V.E., McLinden, C.A., Joiner, J., Krotkov, N.A., Bian, H., Janssens-Maenhout, G., Darmenov, A.S., Silva, A.M. da, 2018. A new global anthropogenic SO_2 emission inventory for the last decade: a mosaic of satellite-derived and bottom-up emissions. Atmospheric Chem. Phys. 18, 16571–16586. https://doi.org/10.5194/acp-18-16571-2018.

Lu, Z., Zhang, Q., Streets, D.G., 2011. Sulfur dioxide and primary carbonaceous aerosol emissions in China and India, 1996–2010. Atmospheric Chem. Phys. 11, 9839–9864. https://doi.org/10.5194/acp-11-9839-2011.

Ma, J., Aardenne, J.A. van, 2004. Impact of different emission inventories on simulated tropospheric ozone over China: a regional chemical transport model evaluation. Atmospheric Chem. Phys. 4, 877–887. https://doi.org/10.5194/acp-4-877-2004.

McLinden, C.A., Fioletov, V., Shephard, M.W., Krotkov, N., Li, C., Martin, R.V., Moran, M.D., Joiner, J., 2016. Space-based detection of missing sulfur dioxide sources of global air pollution. Nat. Geosci. 9, 496–500. https://doi.org/10.1038/ngeo2724.

Oda, T., Maksyutov, S., Elvidge, C.D., 2010. Disaggregation of national fossil fuel CO2 emissions using a global power plant database and DMSP nightlight data. Proc. Asia-Pac. Adv. Netw. 30, 219. https://doi.org/10.7125/APAN.30.24.

Ohara, T., Yamaji, K., Uno, I., Tanimoto, H., Sugata, S., Nagashima, T., Kurokawa, J., Horii, N., Akimoto, H., 2008. Long-term simulations of surface ozone in East Asia during 1980 – 2020 with CMAQ and REAS inventory. Air Pollut. Model. Its Appl. XIX, 136–144. https://doi.org/10.1007/978-1-4020-8453-9_15.

Petersen, Anna Katinka, Brasseur, Guy P., Bouarar, Idir, Flemming, Johannes, Gauss, Michael, Jiang, Fei, Kouznetsov, Rostislav, Kranenburg, Richard, Mijling, Bas, Peuch, Vincent-Henri, Pommier, Matthieu, Segers, Arjo, Sofiev, Mikhail, Timmermans, Renske, Ronald van der, A., Walters, Stacy, Xie, Jianming Xu, Zhou, Guangqiang, 2019. Ensemble forecasts of air quality in eastern China–Part2: evaluation of the MarcoPolo–panda predictions system, version1. Geosci. Model Dev. 12, 1241–1266.

Shen, Y., Zhang, X., Brook, J.R., Huang, T., Zhao, Y., Gao, H., Ma, J., 2016. Satellite remote sensing of air quality in the energy Golden Triangle in Northwest China. Environ. Sci. Technol. Lett. 3, 275–279. https://doi.org/10.1021/acs.estlett.6b00182.

Stohl, A., Aamaas, B., Amann, M., Baker, L.H., Klimont, Z., Kupiainen, K., Heyes, C., 2015. Evaluating the climate and air quality impacts of short-lived pollutants. Atmospheric Chem. Phys. 15, 10529–10566 https://doi.org.

Ummel, K., 2012. Carma revisited: an updated database of carbon dioxide emissions from power plants worldwide. SSRN Electron. J. https://doi.org/10.2139/ssrn.2226505.

Urbanski, S.P., Hao, W., 2010. A Wildland fire emission inventory for the Western United States -uncertainty across spatial and temporal scales. AGU Fall Meeting.
Urbanski, S.P., Hao, W.M., Nordgren, B., 2011. The wildland fire emission inventory: western United States emission estimates and an evaluation of uncertainty. Atmospheric Chem. Phys. 11, 12973–13000. https://doi.org/10.5194/acp-11-12973-2011.
Veefkind, J.P., Haan, J.F.D., Brinksma, E.J., Kroon, M., Levelt, P.F., 2006. Total ozone from the ozone monitoring instrument (OMI) using the DOAS technique. IEEE Trans. Geosci. Remote Sens. 44, 1239–1244. https://doi.org/10.1109/2FTGRS.2006.871204.
Wang, R., Tao, S., Ciais, P., Shen, H.Z., Huang, Y., Chen, H., Shen, G.F., Wang, B., Li, W., Zhang, Y.Y., Lu, Y., Zhu, D., Chen, Y.C., Liu, X.P., Wang, W.T., Wang, X.L., Liu, W.X., Li, B.G., Piao, S.L., 2013. High-resolution mapping of combustion processes and implications for CO_2 emissions. Atmospheric Chem. Phys. 13, 5189–5203. https://doi.org/10.5194/acp-13-5189-2013.
Werf, G.R. van der, Randerson, J.T., Giglio, L., Collatz, G.J., Mu, M., Kasibhatla, P.S., Morton, D.C., DeFries, R.S., Jin, Y., Leeuwen, T.T. van, 2010. Global fire emissions and the contribution of deforestation, savanna, forest, agricultural, and peat fires (1997–2009). Atmospheric Chem. Phys. 10, 11707–11735. https://doi.org/10.5194/acp-10-11707-2010.
Yokelson, R.J., Karl, T., Artaxo, P., Blake, D.R., Christian, T.J., Griffith, D.W.T., Guenther, A., Hao, W.M., 2007. The tropical forest and fire emissions experiment: overview and airborne fire emission factor measurements. Atmospheric Chem. Phys. 7, 5175–5196. https://doi.org/10.5194/acp-7-5175-2007.
Yue, S., Pilon, P., 2011. A comparison of the power of the t test, Mann-Kendall and bootstrap tests for trend detection/Une comparaison de la puissance des tests t de student, de Mann-Kendall et du bootstrap pour la détection de tendance. Hydrol. Sci. J. https://doi.org/10.1623/hysj.49.1.21.53996.
Zhang, Y., Bocquet, M., Mallet, V., Seigneur, C., Baklanov, A., 2012. Real-time air quality forecasting, part II: state of the science, current research needs, and future prospects. Atmos. Environ. 60, 656–676. https://doi.org/10.1016/j.atmosenv.2012.02.041.
Zhao, Y., Nielsen, C.P., Lei, Y., McElroy, M.B., Hao, J., 2011. Quantifying the uncertainties of a bottom-up emission inventory of anthropogenic atmospheric pollutants in China. Atmospheric Chem. Phys. 11, 2295–2308. https://doi.org/10.5194/acp-11-2295-2011.
Zhong, Q., Shen, H., Yun, X., Chen, Y., Ren, Y., Xu, H., Shen, G., Ma, J., Tao, S., 2019. Effects of international fuel trade on global sulfur dioxide emissions. Environ. Sci. Technol. Lett, 727–731 https://doi.org/10.1021/acs.estlett.9b00617.